Anisotropic velocity model calibration with controlled complexity– A microseismic monitoring case study

Junwei Huang, Philip J. Usher

ITASCA Consulting Ltd, Shrewsbury, United Kingdom

Summary

We calibrated a layered Vertical Transversal Isotropic (VTI) velocity model for a 12-stage hydraulic fracturing microseismic monitoring project in the Woodford shale formation. With limited observatioins (P and SH first arrivals) and additonal degrees of freedom (Thomsen parameters) for each layer, the VTI model calibration is an underdetermined problem. To avoid overfitting and local optima, we progressively increased the complexity of the model by first searching for a layered P and S velocity constrained by sonic logs, followed by adding non-zero Thomsen parameters (ε, δ, γ), gamma log constrained Thomsen parameters and finally a general layered velocity model with 5 degrees of freedom (v_p, v_s, ε, δ, γ) in each layer. For computation efficiency, a randomised optimization technique Gaussian Particle Swarm Optimization was employed for global optimum search. We showed that with increasing complexity, the event locations become more accurate with less artefacts and systematic biases. In addition, due to the absence of perforation or ball seating signals, we were able to obtain the calibrated model using microseismic events from early injection episode of multiple stages. This method can be extended to use any microseismic events for velocity calibration and microseismic relocation similar to joint velocity model and hypocenter inversion.

Background

The data set used in this study is from microseismic monitoring of a hydraulic fracturing stimulation in the Woodford shale formation (Smith et al. 2016). As shown in Figure 1, the injection occurred at a depth of 11400 ft (3.5 km) with twelve stages along a horizontal zone of 4500 ft (1.4 km). This was monitored by twelve three-component geophones from 9500 ft (2.9 km) to 10500 ft (3.2 km) deep. A dipole sonic log recorded both P and S wave velocities in the treatment well, above the injection zone. Only one string shot below the monitoring well towards the heel of the treatment well was recorded for velocity model calibration and sensor orientation. Although the completion was a mechanical (sliding sleeve with no perforation shots), no clear ball drop events could be identified. Due to the absence of events with known locations, early microseismic events from each stage were assumed to originate close to the injection location. These microseismic events were manually inspected to verify they had a high signal to noise ratio and were compared with synthetic waveforms, to confirm that to the best of our knowledge the events were located close to the injection point. (Smith et al., 2016).
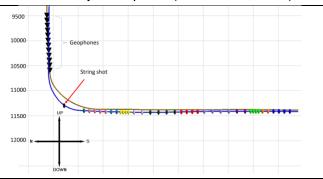

Figure 1: *Location of the string shot used for calibration of velocity model and orientation in the original processing, relative to the array. The string shot is at the heel of the well, with a near vertical ray path and is not ideal for VTI velocity model calibration. The designed sleeve opening positions were in colour.* No clear ball drop events were identified in the project. *Grid: 500 ft.*

Workflow

To locate microseismic events with high accuracy, a velocity model must be calibrated using ray paths similar to the expected microseismicity. As shown in Figure 2, we automated the multi-step velocity calibration method from Usher et al (2018). Each calibration step reduces the traveltime residual between the theoretical arrival and the picked arrivals. For computation efficiency, the randomized optimization technique Gaussian Particle Swarm Optimization (e.g., Krohling 2004) was employed in all steps for global optimum.

1. The P- and S-wave velocities, the number of layers and the boundary of each layer were based on the dipole sonic logs. For each layer, we defined the upper and lower boundary of v_p and v_s and performed a global search for all layers simultaneously to minimie the traveltime residual. The isotropic velocity model can deviate from the sonic logs within limited range. The calibrated isotropic model was used as the starting model for the next step. The layers were fixed in the following steps.
2. A set of constant Thomsen parameters (Thomsen 1986) were searched within a user defined range and both v_p and v_s can be perturbed to further reduce the traveltime residual. In this study, we found $\varepsilon = 0.082$, $\delta = -0.003$, and $\gamma = 0.085$. Given that we were searching within a large range (e.g. from -0.5 to 0.5) for the Thomsen parameters, general transversal isotropy (strong anisotropy) must be modelled.
3. We allowed ε, δ, and γ to vary in depth and assumed that they were linearly proportional to gamma log (Leaney et al 2014). In this step, a set of layer independent constants as well as layered v_p&v_s were searched to minimise the traveltime residual.
4. Finally, we consider 5 degrees of freedom (v_p, v_s, ε, δ, and γ) for each layer and allow independent perturbation. The search space is confined by the previously calibrated model.
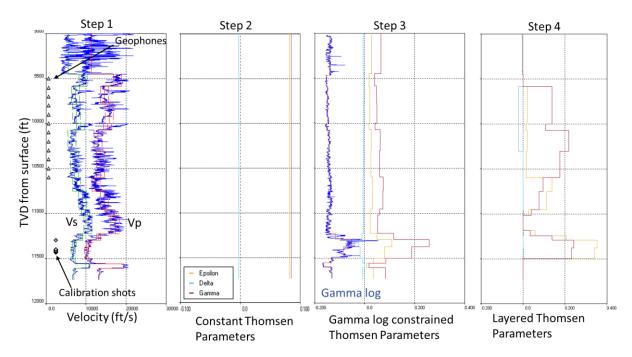

Figure 2: *The velocity models used in this study are; a) a 17-layer isotropic model with perturbation range marked by dashed lines, b) constant Thomsen parameters, c) Thomsen parameters proportional to gamma log (blue curve), d) Layered Thomsen parameters independently optimized for each layer.*

Processing Results

Approximately 6000 microseismic events were located in an area of 5000 ft x 4000 ft (1.5 km x 1.2 km) around the well, from depths of between 10500 ft (3.2 km) and 12000 ft (3.7 km) (Figure 3). All detected

events were located using the calibrated velocity model from each step for comparison (see Figure 3). With increasing complexity of the calibration models, the location accuracy of the events improved as shown by the events clustered around the injection points. The cross-section view shows linear trends for the isotropic velocity model. The separation between these linear trends increases with distance from the array (Figure 3a). For a VTI model with constant Thomsen parameters, the locations were improved with the top artefact removed (Figure 3b). For the velocity model proportional to gamma log, the two trends were still present, and the events systematically spread deeper with distance (Figure 3c). For the model with the separate VTI parameters for each layer, the trends were significantly reduced, and most events were located closer to the depth of the injection well, 11400 ft (3.5 km). The systematic bias, i.e. the increasing variation in depth for events at large offset, was due to inaccurate Thomsen parameters and this is reduced in the last model.
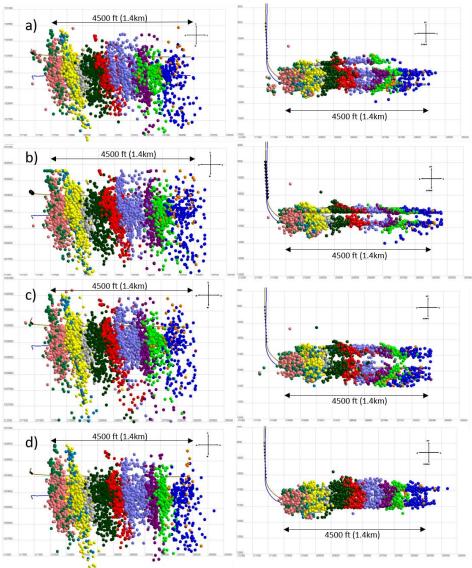

Figure 3: *A map (left) and cross section (right) of the microseismic event locations for each velocity model; a) isotropic model from step 1, b) layered v_p, v_s and constant Thomsen parameters (step 2), c) layered v_p, v_s and gamma log constrained Thomsen parameters, d) layered v_p, v_s and Thomsen parameters. The map view shows an increase in clustering with the increasing complexity of the velocity models. The cross sections show that the linear trends, likely artefacts due to the velocity model, were reduced by increasing the complexity of the velocity structure.*

Using the final velocity model, we can verify that the predicted SH and SV arrivals are consistent with the waveform (see Figure 4). In addition, SV arrivals not picked in this study was used to cross-validate the final model. Depending on the data quality, the SV picks can be included in the velocity calibration for better constraints.
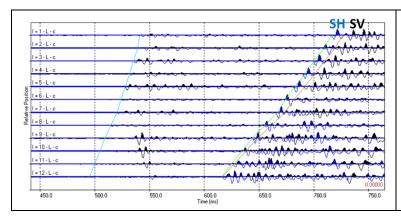

Figure 4: An example waveform showing the shear wave splitting. The SH wave (blue) arrives slightly earlier than the SV wave (black). Note that using the final calibrated velocity model, the theoretical arrival of SV (golden line) is consistent with the observed SV arrivals.

Conclusions

We have proposed a multiple-step anisotropic velocity model calibration method and shown that as the complexity increases, the traveltime residual for the calibration shots as well as the artefacts observed in this dataset are reduced. Specifically, when a set of Thomsen parameters and velocity values are calibrated for each layer, the events are more clustered, linear artefacts with depth are reduced and the events locate closer to the injection depth. This shows that we need to update 5 parameters simultaneously within a confined error space based on previous calibration steps. We have also demonstrated that it is possible to use microseismic events occurred early in the injection episode for velocity calibration. This method can be applied to any microseismic events for velocity calibration and microseismic relocation similar to joint velocity model and hypocenter inversion.

Acknowledgements

References

Krohling, R. A., 2004, Gaussian swarm: a novel particle swarm optimization algorithm: IEEE Conference on Cybernetics and Intelligent Systems, 1, 372–376 vol.1.

Leaney, S., X. Yu, C. Chapman, L. Bennett, S. Maxwell, J. Rutledge, S. Microseismic, J. Duhault, and L. Resources, 2014, Anisotropic moment tensor inversion and visualization applied to a dual well monitoring survey: GeoConvention, 8.

Smith, M. C., S. D. Goodfellow, J. Huang, S. C. Maxwell, J. Teff, B. Kennedy, and B. Bayliss, 2016, Microseismic Quality Control Using Synthetic Seismograms: Proceedings of the 4th Unconventional Resources Technology Conference.

Thomsen, L., 1986, Weak elastic anisotropy: Geophysics, 51, 1954–1966.

Usher, P. J., and J. Huang, 2018 submitted, Improving anisotropic velocity model calibration in microseismic data from the Woodford Shale, Sixth EAGE Shale Workshop, 28 April - 2 May, Bordeaux, France